Entrainment into a Stratocumulus Layer with Distributed Radiative Cooling

DAVID A. RANDALL

Department of Meteorology, Massachusetts Institute of Technology, Cambridge, 02139

(Manuscript received 15 May 1979, in final form 20 August 1979)

ABSTRACT

It is shown that the radiative cooling of a cloud layer strongly influences the turbulent flux profiles and the entrainment rate, and that the radiative cooling should be modeled as acting *inside* the turbulent layer. Numerical experiments demonstrate that a cloud-topped mixed-layer model, similar to that of Lilly (1968), is quite sensitive to δp_R, the depth of the radiatively cooled layer near cloud top. As δp_R increases, the model's sensitivity to the entrainment assumption is markedly heightened. More specifically, for large δp_R the cloud top and cloud base rise dramatically as the entrainment parameter k is increased, while for small δp_R an increase in k has almost no effect. The model is most sensitive to Δp_R precisely for the cold-water, strong-divergence regime of greatest interest.

1. Introduction

Lilly (1968) pointed out the need to understand the extensive, nearly steady marine stratocumulus regimes which commonly fill the upper planetary boundary layer (PBL) off the west coasts of continents, while Herman and Goody (1976) drew attention to the persistent, multiply-layered PBL stratus layers of the summertime arctic. As a result of growing recognition of the importance of these PBL cloud layers, attempts have been made to parameterize PBL stratocumulus processes in the general circulation models under development at UCLA (Randall, 1976) and NCAR (Benoit, 1976). Stratocumulus entrainment is a key process in such parameterization theories.

Entrainment occurs when the interface between a turbulent layer and a quiet layer is not simply advected by the mean circulation, but moves progressively into the quiet layer relative to the mean flow. Because fluid is entrained from a quiet region into a turbulent region, it must be supplied with turbulence kinetic energy (TKE), and whenever the entrainment occurs across a gravitationally stable interface, additional TKE is needed to do work against the stratification. For these reasons, the entrainment process has often been studied in terms of the conservation of TKE.

From this point of view, the cloud-topped PBL is distinguished by its unique vertical distribution of buoyant production of TKE. Whereas the clear PBL is convectively active or suppressed according to whether it is being heated or cooled from below, Lilly (1968) showed that the cloud-topped PBL is nearly always convectively driven by strong radiative cooling from above,[1] sometimes in spite of weak turbulent cooling to underlying cold water. Cloud-layer convection is also favored by condensational warming near the cloud base and evaporative cooling near the cloud top.

Lilly (1968) assumed that the radiative cooling is concentrated in a layer of infinitesimal thickness just above the cloud-top level, and above the limits of the convective turbulence. But Deardorff (1976) pointed out that the convective turbulence will inevitably penetrate into the radiatively cooled layer, since to a large extent the turbulence is *forced* by the cooling. He therefore revised Lilly's model to account for radiative cooling within the convective layer. Still, he allowed a portion of the cooling to occur above the convective layer, and, like Lilly, he assumed that the cooling is confined to a layer of infinitesimal thickness. Recently, Kahn and Businger (1979) have argued that *all* of the cooling occurs within the convective layer and, more importantly, that the cooling is distributed through a layer of finite depth. The latter idea is supported by the observations of Paltridge (1974), Platt (1976) and Herman (1979), which show that the radiative extinction length for thermal radiation in the cloud can be as large as several hundred meters.

Schubert *et al.* (1979) followed the suggestion of Kahn and Businger, by including the effects of radiative cooling in their prediction equation for the mixed layer moist static energy. But they failed to consider that the distribution of radiative cooling

[1] In this paper we discuss only the effects of longwave cooling of the cloud; solar warming is not considered.

0022-4928/80/010148-12$07.00

also influences the shape of the buoyancy flux profile, whose importance in determining the entrainment rate has already been mentioned above. Lilly and Schubert (1980) did consider this effect in a revised model, but they studied only a radiatively cooled "smoky" mixed layer; cloud processes were not included.

Despite the progress reviewed above, the proper distribution of radiative cooling in cloud-topped mixed-layer models and the effects of the cooling on the mixed-layer turbulence continue to be controversial problems. The purpose of this paper is to contribute to the resolution of these problems, giving particular attention to the effects of distributed radiative cooling on the shape of the mixed-layer buoyancy flux profile, and on the entrainment rate.

The plan of the paper is as follows. In Sections 2 and 3, we discuss the entrainment assumption and the relationships among the net radiation flux, the turbulent fluxes and the entrainment rate. Then, in Section 4, we draw on this background to determine the proper vertical distribution of radiative cooling in a mixed-layer model. In Section 5, we discuss approximate analytical relationships between the radiative cooling profile and the entrainment rate. Finally, a numerical model is described in Section 6, and model results are presented in Section 7.

2. The entrainment assumption

Ball (1960) first suggested that the rate of entrainment into the planetary boundary layer (PBL) is determined by the condition that

$$N/P = k^2, \tag{2.1}$$

where gN is the integrated rate of turbulence kinetic energy (TKE) *destruction* due to downward buoyancy flux, gP is the integrated rate of TKE *production* due to upward buoyancy flux, and k^2 is a constant. More precisely, N and P are defined by

$$N \equiv \int_{p_{B+}}^{p_S} \frac{\kappa F_{sv}(p)}{p} [1 - \lambda(p)] dp, \tag{2.2}$$

$$P \equiv \int_{p_{B+}}^{p_S} \frac{\kappa F_{sv}(p)}{p} \lambda(p) dp, \tag{2.3}$$

where $\kappa \equiv R/c_p$, F_{sv} is the turbulent flux of virtual dry static energy, p is pressure, subscripts S and $B+$ denote the surface and a level just above the PBL top, respectively, and

$$\lambda \equiv \begin{cases} 1, & F_{sv}(p) \geq 0 \\ 0, & F_{sv}(p) < 0. \end{cases} \tag{2.4}$$

According to these definitions, N and P are both non-negative, so that k^2 must be non-negative. Ball suggested that $k^2 = 1$, but later studies have shown that $k^2 = 0.04$ is more consistent with observation and numerical experiment.

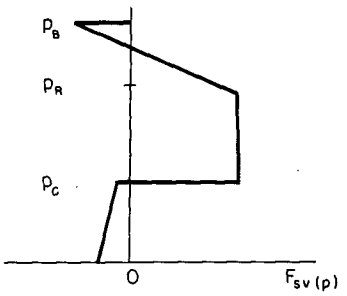

FIG. 1. A schematic illustration of a typical profile of the virtual dry static energy flux in a cloud-topped mixed layer. The cloud-base level p_C, the base of the radiative cooling layer, p_R and the cloud-top level p_B are indicated.

Lilly (1968) applied (2.1) to the cloud-topped mixed layer, considering the two limiting cases $k^2 = 1$ and $k^2 = 0$, which he called "maximum entrainment" and "minimum entrainment," respectively. Schubert (1976) and Kraus and Schaller (1978) suggested interpolations between these limiting cases. This corresponds to a choice of k^2 between zero and one. Of course, Eqs. (2.1)–(2.4) are not sufficiently general to describe all possible modes of stratocumulus entrainment. As discussed by Randall (1979), the definition of P should be generalized to include mechanical production, and (2.1) must be modified to account for that possibility of "free" entrainment, with no negative production.

Still, (2.1) is a plausible entrainment hypothesis for a convective PBL whose entrainment rate is limited by a strong capping inversion. In this paper, we apply (2.1) to the cloud-topped mixed layer, treating k^2 as a parameter.

3. The radiative and turbulent flux profiles of an entraining cloud-topped mixed layer

Fig. 1 schematically illustrates a typical (e.g., Deardorff, 1976; Schubert *et al.*, 1979) profile of $F_{sv}(p)$ for a cloud-topped mixed layer. As discussed in the Introduction, the TKE balance of the cloud-topped PBL is strongly influenced by vigorous buoyant production in the cloud layer, forced by radiative cooling from above and by a combination of condensation warming near cloud base and evaporative cooling near cloud top. Related features of Fig. 1 are the sharp upward increase of F_{sv} near the cloud-base level, and the peculiar "double kink" in $F_{sv}(p)$ near the cloud-top level. In this section, we shall examine these features more carefully. But first we must relate F_{sv} to the turbulent fluxes of moist static energy and moisture, and to the net radiative flux.

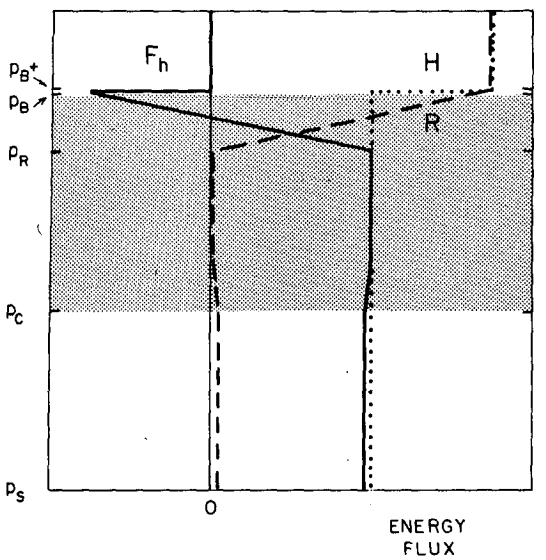

FIG. 2. A schematic illustration of the profiles of the moist static energy flux F_h, the radiation flux R and their sum H, in a cloud-topped mixed layer. The pressures at the surface, cloud base, base of the radiatively cooled layer and cloud top are denoted by p_S, p_C, p_R, p_B and p_{B+}, respectively. For completeness, the possibility of weak radiative warming near cloud base is indicated in the figure, although it is omitted, for simplicity, in the mixed-layer model.

The moist static energy $h \equiv c_pT + gz + Lq$ and the total water mixing ratio $(q + l)$ are convenient variables to work with, because they are conserved under both moist and dry adiabatic processes. The turbulent flux of virtual dry static energy F_{sv} is related to the turbulent fluxes of moist static energy and total water mixing ratio, denoted by F_h and F_{q+l}, respectively, through

$$F_{sv} = F_h - (1 - \delta\epsilon)LF_{q+l}, \tag{3.1}$$

for clear air, and through

$$F_{sv} = \beta F_h - \epsilon LF_{q+l}, \tag{3.2}$$

for uniformly cloudy air (see, e.g., Schubert, 1976). Here $\epsilon \equiv c_pT/L$, $\delta = 0.608$, L is the latent heat of condensation, $\beta \equiv [1 + (1 + \delta)\gamma\epsilon]/(1 + \gamma)$, $\gamma \equiv (L/c_p) \times (\partial q^*/\partial T)_p$, and q^* is the saturation mixing ratio. Randall (1980) generalizes (3.2) for the case of partly cloudy air, and gives plots of β and γ as functions of T and p.

In a mixed layer the total thermodynamic energy flux must obey

$$\partial H/\partial p = (H_S - H_B)/\delta p_M, \tag{3.3}$$

where

$$H \equiv F_h + R, \tag{3.4}$$

R is the net radiative flux, and δp_M is the pressure depth of the PBL. Similarly, the total moisture flux must obey

$$\frac{\partial}{\partial p}(F_{q+l}) = [(F_{q+l})_S - (F_{q+l})_B]/\delta p_M. \tag{3.5}$$

From (3.3) and (3.5), we see that $\partial H/\partial p$ and $\partial/\partial p(F_{q+l})$ are independent of height. At any level inside the mixed layer, F_h can be obtained from

$$\begin{aligned} F_h(p) &= H_S - (p_S - p)\partial H/\partial p - R(p) \\ &= H_S\left(\frac{p - p_B}{\delta p_M}\right) \\ &\quad + H_B\left(\frac{p_S - p}{\delta p_M}\right) - R(p). \end{aligned} \tag{3.6}$$

Here the second equality has been obtained by use of (3.3). Similarly, we can obtain F_{q+l} at any level inside the mixed layer from

$$\begin{aligned} F_{q+l}(p) &= (F_{q+l})_S\left(\frac{p - p_B}{\delta p_M}\right) \\ &\quad + (F_{q+l})_B\left(\frac{p_S - p}{\delta p_M}\right). \end{aligned} \tag{3.7}$$

Fig. 2 schematically summarizes the relationships between the profiles of H, F_h, and the net radiative flux R. In the figure, level R lies at the base of the layer of strong radiative cooling, well inside the cloud layer; level B lies at the top of the radiatively cooled layer, just inside the cloud; and level $B+$ lies in clear air, just above the PBL top, where all turbulent fluxes vanish. For simplicity, the figure illustrates a situation in which H is uniform throughout the mixed layer; changes in F_h are therefore accompanied by equal but opposite changes in R. This rule is violated between levels B and $B+$ (i.e., at the mixed-layer top), where H and F_h increase discontinuously with height, while R changes smoothly. In particular, $\Delta R \equiv R_{B+} - R_B = 0$. This important assumption, which follows the recommendation of Kahn and Businger (1979), is justified at length in the next section. Also, we assume for simplicity and computational economy that R varies linearly with p from p_R to p_B. (Admittedly, an exponential height dependence might be more realistic.)

The conservation law for h, evaluated for the thin layer B–$B+$, can be expressed as

$$\Delta H = E\Delta h. \tag{3.8}$$

Here E is the entrainment mass flux. Since R is continuous, ΔH is associated with the sudden change of F_h from its (generally nonzero) value at B to zero at $B+$. An alternative form of (3.7) is thus

$$(F_h)_B = -E\Delta h. \tag{3.9}$$

We can now understand the double-kink structure of $F_h(p)$, shown in Fig. 2: the lower kink is associated with radiative cooling and the upper kink is associ-

ated with the entrainment of high-energy air. By analogy with (3.9), we find that the moisture flux at level B must satisfy

$$(F_{q+l})_B = -E\Delta(q + l). \tag{3.10}$$

Use of Eqs. (3.9)–(3.10) in (3.6)–(3.7) allows us to expose the influence of entrainment on the turbulent flux profiles in the mixed-layer interior:

$$F_h(p) = H_S\left(\frac{p - p_B}{\delta p_M}\right) + R_B\left(\frac{p_S - p}{\delta p_M}\right) - R(p) - E\Delta h\left(\frac{p_S - p}{\delta p_M}\right), \tag{3.11}$$

$$F_{q+l}(p) = (F_{q+l})_S\left(\frac{p - p_B}{\delta p_M}\right) - E\Delta(q + l)\left(\frac{p_S - p}{\delta p_M}\right). \tag{3.12}$$

These results show that for each p, F_h and F_{q+l} depend linearly on E.

We are now in a position to understand the various features of Fig. 1, beginning with the discontinuity in F_{sv} at cloud base. As can be seen from (3.6)–(3.7), the profiles of F_h and F_{q+l} are both continuous at cloud base, because h and $(q + l)$ are both conserved during moist adiabatic as well as dry adiabatic processes, and, therefore, both may be well-mixed by turbulence in spite of phase-change processes in a cloud layer. But Lilly (1968) pointed out that, because the virtual dry static energy is not conserved during moist adiabatic processes, there can be a near-discontinuity in F_{sv} at cloud base. By applying (3.2) just above cloud base and (3.1) just below cloud base, and subtracting, we find that

$$(F_{sv})_{C+} - (F_{sv})_{C-} = [1 - (1 + \delta)\epsilon]L(F_l)_{C+}. \tag{3.13}$$

Here the subscripts $C+$ and $C-$ denote levels just above and just below cloud base, respectively. This shows that F_{sv} increases discontinuously upward when there is an upward flux of liquid into the cloud, as must be the case for a stratus layer which is not decaying. (Of course, in nature the irregular character of cloud base will ensure that F_{sv} changes smoothly, though quickly, there.) The upward increase in F_{sv} at p_C allows $P > 0$ [see Eq. (2.3)], even though $F_{sv} < 0$ in the subcloud layer. In such situations, the subcloud-layer turbulence must be maintained against dissipation mainly by turbulence kinetic energy imported from above. The subcloud-layer turbulence is by no means passive, however; it plays the crucial role of supplying moisture to the cloud layer. Unless this moisture supply is maintained, the cloud layer will be progressively evaporated by dilution with dry, warm entrained air.

The variation of $F_{sv}(p)$ near the PBL top is strongly influenced by both intense radiative cooling and the rapid evaporation of cloud liquid into entrained air. Since $F_{sv}(p)$ is related to $F_h(p)$ through (3.1)–(3.2), the double kink in $F_{sv}(p)$, shown in Fig. 1, is now easily explained in terms of the double kink in $F_h(p)$. Recall that the latter is due to a combination of radiative cooling and the entrainment of high-energy air. Randall (1980) has shown that cooling due to the evaporation of cloud drops into entrained air tends to increase F_{sv} in the upper cloud layer. The effects of entrainment on $(F_{sv})_B$ can be seen by using (3.9)–(3.10) in (3.2), to obtain

$$(F_{sv})_B = -E[\beta\Delta h - \epsilon L\Delta(q + l)]. \tag{3.14}$$

Randall (1980) argues that

$$\beta\Delta h - \epsilon L\Delta(q + l) > 0 \tag{3.15}$$

is required for a stable stratocumulus layer, and we restrict ourselves to such stable layers in this paper. Since $E > 0$, it follows that $(F_{sv})_B < 0$.

Inspection of Figs. 1 and 2 reveals that the decrease of F_{sv} from a positive value at level R to a negative value at level B is a consequence of the fact that the radiative cooling occurs *inside* the cloud layer. This was first understood by Deardorff (1976); negative values of $(F_{sv})_B$ played a key role in his entrainment hypothesis. But Deardorff assumed that the mixed-layer radiative cooling is concentrated in an infinitesimally thick layer; if this were true, it would follow that negative values of F_{sv} near the cloud-top level would be similarly confined.

This is an important point, because negative values of F_{sv} can contribute to N only if they are distributed through a layer of finite thickness. In other words, an appreciable contribution to N can arise near the cloud top level only if the radiative cooling is distributed through a finite depth, i.e., if $\delta p_R \equiv p_R - p_B$ is positive. If $\delta p_R \approx 0$, then N must be entirely due to negative values of F_{sv} in the subcloud layer, as in the theories of Lilly (1968) and Schubert (1976). But for $\delta p_R > 0$, we can have $N > 0$, even though $F_{sv} \geq 0$ throughout the subcloud layer.

Does this actually happen? The second-order closure results of Oliver *et al.* (1978) show $F_{sv} > 0$ at all levels except near cloud top. Lenschow (1973) reported aircraft-observed negative values of F_{sv} in the upper cloud-topped PBL over the Great Lakes. These studies tend to support the hypothesis that distributed radiative cooling allows a significant contribution to N near the cloud top level. More thorough observational verification must await detailed analysis of the data gathered in the California Stratus Experiment (Wakefield and Schubert, 1976).

For later convenience, one last point should be made before closing this section. Combining (3.11)–(3.12) with (3.1)–(3.2), we find that

$$F_{sv}(p) = H_S\left(\frac{p - p_B}{\delta p_M}\right) + R_B\left(\frac{p_S - p}{\delta p_M}\right) - R(p)$$
$$- (1 - \delta\epsilon)L(F_{q+l})_S\left(\frac{p - p_B}{\delta p_M}\right) - E[\Delta h - (1 - \delta\epsilon)L\Delta(q + l)]\left(\frac{p_S - p}{\delta p_M}\right) \quad (3.16)$$

below cloud base and

$$F_{sv}(p) = \beta\left[H_S\left(\frac{p - p_B}{\delta p_M}\right) + R_B\left(\frac{p_S - p}{\delta p_M}\right) - R(p)\right]$$
$$- \epsilon L(F_{q+l})_S\left(\frac{p - p_B}{\delta p_M}\right) - E[\beta\Delta h - \epsilon L\Delta(q + l)]\left(\frac{p_S - p}{\delta p_M}\right) \quad (3.17)$$

above cloud base. We wish to argue that the entrainment terms of (3.16)–(3.17) always tend to decrease F_{sv}; it suffices to show that the bracketed quantities of the entrainment terms are positive. Let's ignore, for the moment, the fact that ϵ and β are weakly dependent on height in the mixed layer (by virtue of their dependence on T and p). Then inequality (3.15) implies that the entrainment term of (3.17) is always negative. Randall (1980) shows that (3.15) implies that Δs_v is strongly positive. It follows that the bracketed quantity in the entrainment term of (3.16) is positive, so that, again, the entrainment term itself is always negative. We can show that the weak height dependence of ϵ and β does not vitiate these conclusions. We have thus shown that the entrainment terms of (3.16) and (3.17) are always negative. If E is increased parametrically, holding the other variables fixed, then at every level in the mixed layer F_{sv} will decrease linearly. This result is used in Section 6.

4. Where does radiation cool?

As reviewed in the Introduction, there has been some disagreement among modelers of cloud-topped mixed layers concerning the proper way to vertically distribute the radiative cooling. Various suggestions range from that of Lilly (1968), who put all of the cooling "in the inversion," to that of Kahn and Businger (1979), who put it all inside the mixed layer. In Section 3, we followed the suggestion of Kahn and Businger, and we now undertake to explain why.

Let's begin the discussion by putting aside mixed-layer models, and thinking instead about real stratocumulus layers. Deardorff (1976) has argued convincingly that the penetration of cloud hummocks into the inversion ensure that at least part of the radiative cooling occurs inside the inversion, above the mixed layer. Here the inversion is defined as the layer in which the horizontally averaged (or ensemble averaged) temperature increases sharply with height. Whether or not an appreciable fraction of the cooling occurs below the inversion depends on the ratio of the inversion depth to the radiative extinction length—a ratio which may be highly variable. Possibly there are cases in which most of the cooling is inside the inversion.

On the other hand, it is clear that *all of the radiative cooling occurs inside the turbulence*, which, in the horizontally averaged sense, extends up to at least the level of the highest cloud tops (James, 1959). Now in the transformation from real stratocumulus layer to idealized mixed-layer model, it is possible to preserve the relationship between the radiative cooling and features of the temperature profile, e.g., by putting the cooling inside the inversion. It is also possible to preserve the relationship between the radiative cooling and the turbulence, e.g., by putting the cooling inside the layer of negative buoyancy flux. But it is not possible to do both at the same time, because the mixed-layer model is too highly idealized.

Fortunately, there is no *need* to do both at the same time, because from the point of view of the mixed-layer temperature equation it doesn't matter whether the radiative cooling is inside the mixed layer or inside the inversion, or shared between them. This can be seen from the conservation law for the mixed-layer moist static energy h_M:

$$\frac{\delta p_M}{g}\frac{dh_M}{dt} = (F_h)_S + R_S - (F_h)_B - R_B$$
$$= (F_h)_S + R_S + E\Delta h - R_{B+}. \quad (4.1)$$

The second equality of (4.1) follows from

$$(F_h)_B = -E\Delta h + \Delta R, \quad (4.2)$$

which is (3.8) generalized to allow the *possibility* $\Delta R \neq 0$. From (4.1), it is clear that for given values of δp_M, $(F_h)_S$, R_S, E, Δh, and R_{B+}, the time rate of change of h_M is fully determined; the value of ΔR is irrelevant.

This frees us to preserve the relationship between the radiative cooling and the turbulence, and the discussion of Section 3 shows that it is important to do so, since the depth of the radiatively cooled layer strongly influences the value of N. To allow this influence, we have to put the cooling inside the turbulence. In the context of an idealized mixed-layer model, this means putting the cooling "inside the mixed layer," but this terminology is misleading and should be avoided.

5. Some special cases

We now use the ideas developed in Section 3 to study analytically some possible modes of entrainment into the stratocumulus-topped PBL. These possibilities are offered as examples; others exist.

a. Negative production near cloud top

Suppose that negative values of F_{sv} occur in the layer between p_R and p_B, but not elsewhere. Defining p_0 as the level where $F_{sv} = 0$ (see Fig. 3a), we have

$$(p_0 - p_B)/\delta p_R = -(F_{sv})_B/[(F_{sv})_R - (F_{sv})_B], \quad (5.1)$$

so that

$$N \approx -\frac{\kappa}{2}\frac{(p_0 - p_S)}{p_B}(F_{sv})_B = \frac{\kappa}{2}\frac{\delta p_R}{p_B}\left[\frac{(F_{sv})_B^2}{(F_{sv})_R - (F_{sv})_B}\right]. \quad (5.2)$$

This is proportional to the shaded area in Fig. 3a. In deriving (5.2), and throughout this section, we use the fact that p varies by only a few percent through the depth of the mixed layer. Rewriting our entrainment assumption (2.1) as

$$N = \left(\frac{k^2}{1 - k^2}\right)(P - N), \quad (5.3)$$

and using (2.2)–(2.3) and (5.2), we find that

$$\frac{1}{2}\delta p_R\left[\frac{(F_{sv})_B^2}{(F_{sv})_R - (F_{sv})_B}\right] \approx \left(\frac{k^2}{1 - k^2}\right)\int_{p_{B+}}^{p_S} F_{sv}dp. \quad (5.4)$$

As shown in Section 3, we can express $F_{sv}(p)$ as a linear function of E for each p. We can therefore derive from (5.4) a quadratic equation which can be solved for E. Unfortunately, the form of the solution is so complicated that it gives little insight into the entrainment process; we do not present it here.

Nevertheless, we can conclude directly from (5.2) that the entrainment rate will depend strongly on δp_R. It is therefore important to determine δp_R accurately, both in modeling applications and in observational tests of the theory. This is discouraging on both counts. Accurate modeling of radiative transfer in the cloud layer will surely require accurate knowledge of both fractional cloudiness and the cloud liquid water profile by drop size (e.g., Kuriyan and Mitra, 1979); mixed-layer models are not well-suited to supply such information. High-resolution profiling of the radiative flux in a cloud layer is certainly a difficult observational task, which might be feasible only with tethered balloons. But simultaneous, detailed measurements of the radiative and turbulent flux profiles in the upper cloud layer would be very useful at this stage of our work.

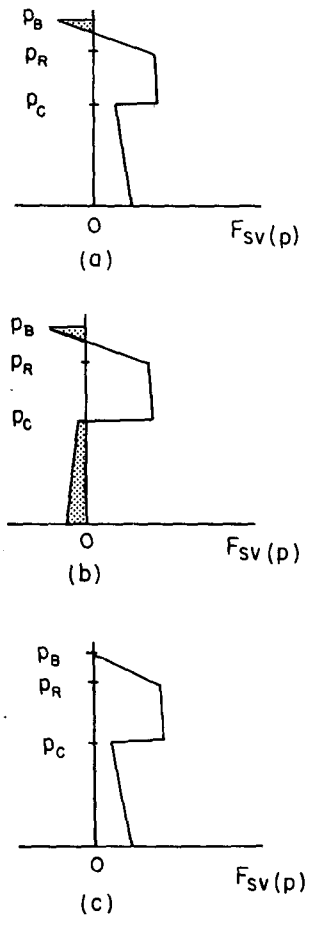

FIG. 3. Three special cases of the F_{sv} profile: (a) negative values only near cloud top; (b) negative values both near cloud top and below cloud base; (c) no negative values. In parts (a) and (b), the region of negative F_{sv} is stipled.

Relation (5.4) is somewhat similar to the "forced stratocumulus entrainment" formula suggested by Deardorff (1976). His proposal was essentially that $(F_{sv})_B$ is a constant times the vertically averaged value of F_{sv}. However, he asserted that this relation holds even if negative values of F_{sv} occur in the subcloud layer, and this is inconsistent with our assumption (2.1).

b. Negative production both near cloud top and below cloud base

When negative production occurs both near the cloud top and throughout the entire subcloud layer (Fig. 3b), we must replace (5.2) by

$$N \approx \frac{\kappa}{2}\frac{\delta p_R}{p_B}\left[\frac{(F_{sv})_B^2}{(F_{sv})_R - (F_{sv})_B}\right] + \frac{\kappa}{2}\left(\frac{p_S - p_C}{p_S}\right)[(F_{sv})_S + (F_{sv})_{C-}]; \quad (5.5)$$

this is proportional to the shaded area in Fig. 3b. The results of Section 3 can be used to obtain a

quadratic equation for E from (5.3) and (5.5), but again the result is too complicated to be very useful. A still more complicated cubic equation for E is obtained for the case in which F_{sv} changes sign in the subcloud layer.

When the subcloud layer is deeper than the layer of radiative cooling, N responds more sensitively to a change in the subcloud-layer buoyancy flux than to a change in the buoyancy flux near cloud top. For this reason, we expect the PBL structure to be relatively insensitive to δp_R when negative production occurs in a deep subcloud layer. In this special case, we therefore expect to obtain results similar to those of Schubert *et al.* (1979).

c. *Very thin clouds*

A noteworthy prediction of the stratocumulus entrainment theory of Deardorff (1976) is that the entrainment rate changes discontinuously in the transition between clear skies and a very thin solid stratocumulus layer. Deardorff points out that, in nature, a very thin solid sheet of cloud probably never occurs; the fractional cloudiness of thin clouds is always fairly small. Fractional cloudiness, which is not included in Deardorff's theory, would then smooth out the evolution of E as clouds formed or dissipated.

We don't dispute the assertion that thin clouds are generally broken clouds, but it nevertheless seems strange that the entrainment rate of a PBL topped by a *hypothetical* infinitesimally thick solid stratocumulus layer would be sharply different from that of a slightly drier but otherwise identical clear PBL. Because we are using (2.1), the influence of the cloud layer is weighted in our theory, through vertical integration, by the cloud depth. As a result, a thin cloud's influence is small, and thus the entrainment rate changes continuously as clouds form or dissipate.

d. *No negative production*

It is clear that any model based on (2.1) will always try to make $N > 0$; if this is impossible for some reason, the model will simply blow up. But Deardorff (1974) has found that when the *clear* PBL deepens through an isentropic layer, no negative production occurs, and deepening is very rapid. For the cloud-topped PBL, an analogous situation could arise for $\beta\Delta h - \epsilon L\Delta(q + l) \leqslant 0$ [see Eq. (3.10)]; a schematic illustration is given in Fig. 3c. To explore this possibility, it is necessary to generalize (2.1) to a more complete expression of the conservation of TKE. Randall (1980) gives further discussion.

6. The mixed-layer model

We now present a simple mixed-layer model, designed to allow tests of the sensitivity of a cloud-topped mixed layer to δp_R. The model is very similar to that discussed by Schubert *et al.* (1979), so only a brief description is given here.

The prognostic equations of the model express the conservation laws for the mixed layer moist static energy, total mixing ratio and mass. These are given by

$$\partial h_M/\partial t = [\rho_S c_T |\mathbf{V}_M|(h^*_{SS} - h_M) - (F_h)_B + R_S - R_B]g/\delta p_M, \quad (6.1)$$

$$\partial(q + l)_M/\partial t = \{\rho_S c_T |\mathbf{V}_M|[q^*_{SS} - (q + l)_M] - (F_{q+l})_B\}g/\delta p_M, \quad (6.2)$$

$$\frac{\partial}{\partial t}(\delta p_M) = -D_M \delta p_M + gE. \quad (6.3)$$

Here h_M and $(q + l)_M$ are the mixed-layer moist static energy and total mixing ratio, respectively; $\rho_S c_T|\mathbf{V}_M|$ is a prescribed "ventilation factor"; and D_M is the prescribed large-scale divergence. The effective sea surface saturation moist static energy h^*_{SS} and the sea surface saturation mixing ratio q^*_{SS} are evaluated using an assumed sea surface temperature and a surface pressure of 1020 hPa.

Following Schubert *et al.* (1979), the free-atmospheric profiles of h and q are assumed to be such that

$$h_{B+} = h_{00} + \Gamma_h \delta z_M, \quad (6.4)$$

$$q_{B+} = q_{00} + \Gamma_q \delta z_M, \quad (6.5)$$

where h_{00}, q_{00}, Γ_h and Γ_q are prescribed, and δz_M is the geometrical depth of the mixed layer, which is hydrostatically determined from the predicted value of δp_M by a method described in Appendix A. The jumps are obtained from

$$\Delta h = h_{B+} - h_M \quad (6.6)$$

and

$$\Delta(q + l) = q_{B+} - (q + l)_M. \quad (6.7)$$

The net radiation flux profile is given as follows. For simplicity, we take $R_S = 0$, since only the net radiative flux divergence matters. The net radiative flux divergence across the mixed layer, $R_S - R_B$, is prescribed, and is assumed to occur entirely within a layer immediately below cloud top. The pressure thickness of this radiatively cooled layer is the prescribed value of δp_R, or the cloud depth, whichever is smaller. The resulting R profile is piecewise linear in p, and is similar to that shown in Fig. 2, except that the weak cloud base warming shown in the figure is neglected in the model, for simplicity.

The cloud base level is determined by a method described in Appendix A.

As indicated in (6.1)–(6.2), the surface fluxes of h and $q + l$ are obtained by a bulk aerodynamic method. Suppose now that E is known. Then $(F_h)_B$ and $(F_{q+l})_B$ can be determined from (3.9) and (3.10), respectively.

All that remains is to determine the entrainment rate and this is accomplished by enforcing (2.1). From (3.16–17), $F_{sv}(p)$ can be obtained for a given value of E. Suppose that the calculation is carried out for $E = 0$. The resulting F_{sv} profile can be vertically integrated to obtain N and P, using straightforward finite difference approximations given in Appendix B. Say that N/P is found to be less than k^2. We can revise our estimate of E by noting that, as E is increased, N/P must increase because N increases and P decreases. This follows from the fact that, as E increases, F_{sv} decreases at every level (see the discussion at the end of Section 3). We can thus make N/P as large as necessary by increasing E. There will be one and only one value of E such that $N/P = k^2$. We determine this value iteratively.

But it is possible that, for $E = 0$, N/P is already greater than k^2. This can happen for very cold sea surface temperatures or for very weak radiative cooling. In such cases the entrainment assumption of Section 2 is inappropriate and the generalizations discussed by Randall (1979) must be introduced. In the present study no such complications arise.

7. Numerical results

In this section, we present equilibrium solutions obtained by time marching with (6.1)–(6.3) for 50 days, by which time a nearly steady state is reached. The radiation flux R is assumed to be zero for $p \geq p_R$,

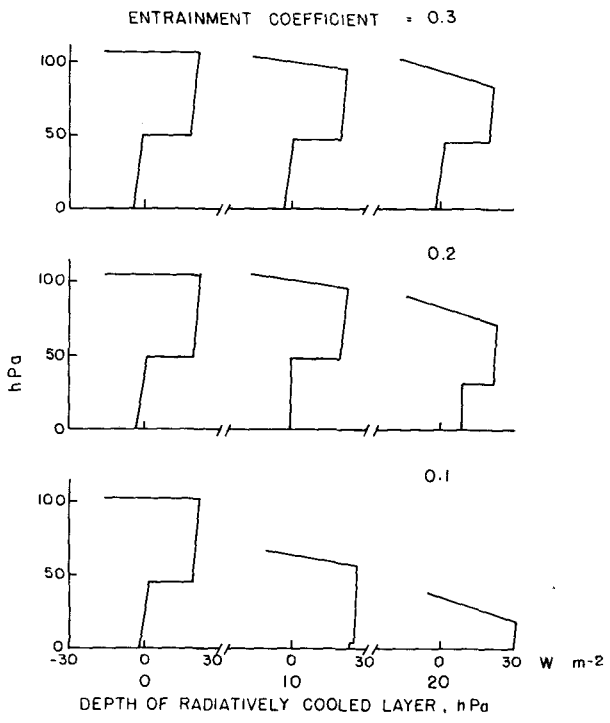

FIG. 4. Profiles of F_{sv} (W m^{-2}) obtained for $k = 0.1$, 0.2, 0.3, and $\delta p_R = 0$, 10, 20 hPa. The values of all other parameters are given in the text.

TABLE 1. The evaporation rate (mm day^{-1}) as a function of δp_R and k for $T_{SS} = 15$°C and $D_M = 4 \times 10^{-6}$ s^{-1}.

	δp_R (hPa)		
k	0	10	20
0.1	1.8	1.3	0.3
0.2	1.9	1.9	1.6
0.3	1.9	1.9	1.9

and to increase linearly to 70 W m^{-2} for $p_R \leq p \leq p_B$. In this study, we assume throughout that $h_{00} = 314.4$ k J kg^{-1}, $\Gamma_h = 1.87$ J kg^{-1} m^{-1}, $q_{00} = 4.38$ g kg^{-1}, $\Gamma_q = -0.614 \times 10^{-6}$ g kg^{-1} m^{-1}, and $\rho_s c_T |\mathbf{V}_M| = 1.26 \times 10^{-2}$ kg m^{-2} s^{-1}. These values are consistent with the "Oakland" case discussed by Schubert *et al.* (1979). In all cases, the assumed initial conditions are $h_M = 3.07 \times 10^5$ J kg^{-1}, $(q + l)_M = 8.3$ g kg^{-1} and $\delta p_M = 150$ hPa. We vary the sea surface temperature T_{SS}, the divergence D_M, the entrainment coefficient k and the depth of the radiative cooling δp_R as parameters.

Fig. 4 shows the profile of $F_{sv}(p)$ for each of the nine cases obtained for $k = 0.1$, 0.2, 0.3 and $\delta p_R = 0$, 10, 20 hPa. It has been assumed that $D_M = 4 \times 10^{-6}$ s^{-1} and $T_{SS} = 15$°C. The figure shows that sensitivity to δp_R is slight for $k = 0.3$, but is quite noticeable for $k = 0.2$, and is spectacular for $k = 0.1$. As δp_R is increased, for fixed k, the PBL top and the cloud base level both drop toward the sea surface, while F_{sv} increases everywhere except inside the radiatively cooled layer. These results are in general agreement with the predictions of Lilly and Schubert (1979). They can be interpreted as follows.

The discussions of Sections 3 and 5, and particularly the relations (5.2) and (5.5), show that, for a given value of E, N increases as δp_R increases. But the entrainment condition (2.1) states that the ratio of N to P is fixed. So if a solution valid for $\delta p_R = 0$ is upset by allowing $\delta p_R > 0$, the model can respond by decreasing E, thus tending to avoid an increase in N, *or* by increasing P, or both. Inspection of Fig. 4 shows that, in fact, both options are exercised. The reduction in PBL depth as δp_R is increased reflects a corresponding reduction in E [see Eq. (6.3)], while the accompanying shift of the F_{sv} profile toward larger values is associated with an increase in P.

From (3.9), we see that a reduction in E will favor a reduction in $(F_{q+l})_B$. But F_{q+l} must be uniform with height in equilibrium, so $(F_{q+l})_S$ will decrease too. Table 1 documents this reduction, which is particularly noticeable for $k = 0.1$. Since the evaporation rate satisfies a bulk aerodynamic formula, a reduction in the evaporation rate must be accompanied by an increase in $(q + l)_M$.

Since $(F_{q+l})_S$ decreases as δp_R increases, the increase in $(F_{sv})_S$ must be due to an increase in the

surface sensible heat flux. In view of the bulk aerodynamic formulae, the PBL must therefore be colder. But in a colder, wetter PBL, the cloud base will, of course, be lower. So even though the cloud top lowers, the cloud depth remains relatively unchanged. This favors an increase in P, since the largest values of F_{sv} occur in the cloud layer.

It is clear that, for a given increment in N, the increment in P needed to satisfy (2.1) increases sharply in magnitude as k is reduced. This is why the mixed layer is particularly sensitive to δp_R for small k. Another point of view is that the mixed layer's sensitivity to k is much greater for $\delta p_R > 0$ than for $\delta p_R = 0$.

We now fix k at 0.2, and ask how the mixed layer's sensitivity to δp_R varies with T_{SS} and D_M. Fig. 5 shows how the profile of $F_{sv}(p)$ changes as T_{SS} is varied from 13 to 18°C, and as D_M is varied from 1×10^{-6} to 6×10^{-6} s^{-1}. The reduction in $(F_{a+l})_S$ which accompanies an increase in δp_R is plotted in the D_M-T_{SS} plane in Fig. 6. The general nature of the response of the mixed layer to an increase in δp_R is qualitatively the same as that shown earlier in Fig. 4 and Table 1. Sensitivity to δp_R is strong for cold water and large divergence, and is negligible for warm water and small divergence. Climatologically, PBL stratocumulus layers are very often found over cold water in regions of strong divergence (e.g., Schubert *et al.*, 1979), so that sensitivity to δp_R is greatest for just those conditions which have the greatest real-world relevance. The variation in sensitivity seen in Figs. 5 and 6 can be interpreted in terms of the ratio $\delta p_R/\delta p_M$. Where the mixed layer is deep, so that this ratio is small, a

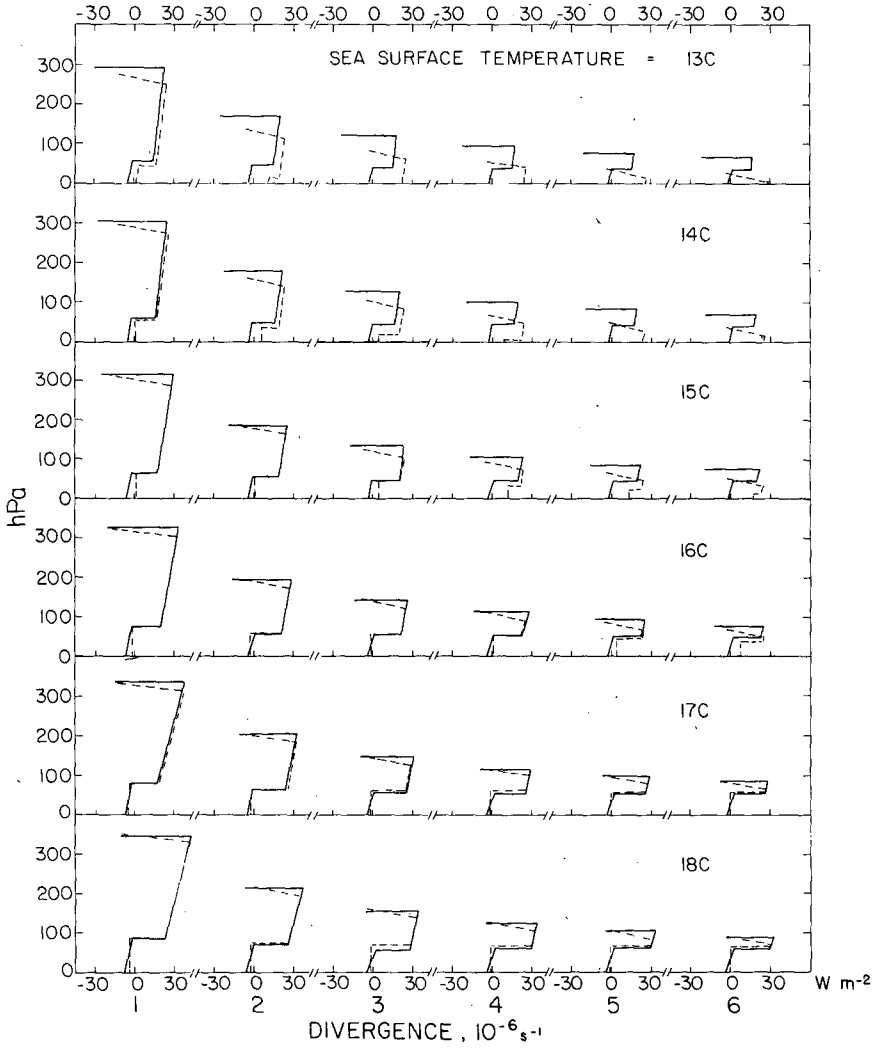

FIG. 5. Profiles of F_{sv} (W m^{-2}) for $k = 0.2$, varying D_M from 1×10^{-6} to 6×10^{-6} s^{-1}, and varying T_{SS} from 13 to 18°C. The solid and dashed lines are for $\delta p_R = 0$ and 20 hPa, respectively.

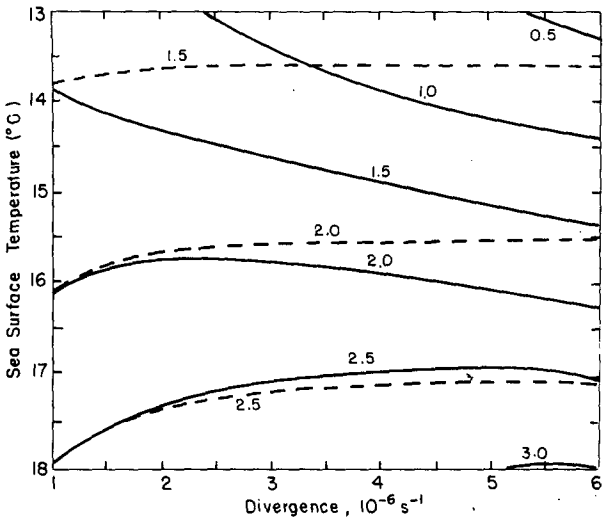

FIG. 6. Variation of the evaporation rate (mm day^{-1}) with sea surface temperature and large-scale divergence. Solid lines are for $\delta p_R = 20$ hPa, while dashed lines are for $\delta p_R = 0$.

very slight increase in F_{sv} over the bulk of the mixed layer is sufficient to balance the increase in δp_R. But where the mixed layer is shallow, so that $\delta p_R/\delta p_M$ is relatively large, drastic changes in the mixed-layer structure are required to balance increased negative production.

8. Conclusions and discussion

We have demonstrated that cloud-topped mixed-layer structure is sensitive to the depth of the layer of radiative cooling near cloud top; and that this sensitivity is greatest over cold water, with strong divergence, and for small values of the entrainment coefficient. More specifically, the principal effects of an increase in the depth of the radiatively cooled layer are to lower both cloud top and cloud base toward the sea surface, and to increase the buoyancy flux at all levels below the base of the radiatively cooled layer. Furthermore, the sensitivity of the mixed layer structure to details of the entrainment parameterization is greatly increased as the depth of the radiatively cooled layer increases.

These results have a number of implications for the future course of theoretical and observational studies of stratocumulus convection. First of all, the comforting result that cloud-topped mixed-layer structure is insensitive to the details of the entrainment assumption, reported by Lilly (1968) and Schubert (1976), is now seen to be valid only for the special case of small δp_R. It follows that much more careful consideration must be given to entrainment assumptions like (2.1); is there really any reason to suppose that k is a constant? Analysis of results from higher order closure models (e.g., Oliver *et al.*, 1978) and Deardorff's three-dimensional turbulence model may help us here, but there can be no substitute for a detailed observational study of marine stratocumulus convection.

Turbulence and radiation measurements must share the highest priority in such a field experiment; the cloud top region should receive special attention. In addition, cloud microphysical data would greatly facilitate interpretation of the radiation data. Finally, the measurement of the local tendency and divergence terms of (6.3) would allow the entrainment rate to be determined as a residual; of course, measurement of the divergence would entail boundary-layer wind profiling at a minimum of three stations.

Acknowledgments. Helpful conversations with Drs. D. Lilly, J. Deardorff, W. Schubert and G. Herman are gratefully acknowledged. This work was sponsored by the National Aeronautics and Space Administration under Grant NGR 22-009-727.

APPENDIX A

Cloud Depth and Thermodynamic Coefficients

To obtain the PBL depth δz_M, which is needed in (5.4) and (5.5), we use the hydrostatic relation

$$\delta z_M = \delta p_M/(g\rho_M), \tag{A1}$$

and let

$$\rho_M = \tfrac{1}{2}(\rho_S + \rho_B), \tag{A2}$$

where

$$\rho_S = \frac{p_S}{\kappa C_p T_S}, \tag{A3}$$

$$\rho_B = \frac{p_B}{\kappa C_p T_B}, \tag{A4}$$

$$T_S = [h_M - L(q + l)_M]/C_p, \tag{A5}$$

$$T_B = [h_M - g\delta z_M - L(q + l)_M]/C_p. \tag{A6}$$

For simplicity, we have neglected the possible connection to (A5) which is required in the presence of a surface layer. We have also neglected the liquid, if any, at the surface and at the PBL top, for the purpose of computing T_S and T_B. This is justified, since liquid water mixing ratios are typically one to two orders of magnitude smaller than vapor mixing ratios (e.g., Neiburger, 1949; Herman and Goody, 1976). Simultaneous solution of (A1)–(A6) gives

$$T_B = [b + (b_2 + p_S p_B)^{1/2}]/\rho_S \kappa C_p, \tag{A7}$$

where

$$b \equiv (\tfrac{1}{2} - \kappa)\delta p_M. \tag{A8}$$

Once T_B is known from (A7), we find ρ_B, ρ_M, and δz_M by using (A4), (A2) and (A1), in turn.

The cloud depth is determined as follows: Let

$$\hat{l}(p) \equiv (q + l)_M - q^*(T,p); \tag{A9}$$

where $\hat{l} \geq 0$, it is equal to the liquid water mixing ratio l; otherwise $l = 0$. We first check $\hat{l}_B$. If it is negative or zero, we have no cloud. For $\hat{l}_B > 0$, we assume that $\hat{l}$ varies linearly from the surface to the PBL top, and that the cloud base is the intermediate level where $\hat{l} = 0$ (if such a level exists) or the earth's surface (otherwise). It follows that

$$p_C - p_B = \delta p_M \,\mathrm{Max}\left\{1, \frac{(q + l)_M - q_B^*}{q_S^* - q_B^*}\right\} . \quad \text{(A10)}$$

The height variation of the thermodynamic coefficients γ and ϵ is taken into account by evaluating these functions in terms of the temperatures and pressures at the levels S, C, R and B where they are needed. The methods for determining T_S, T_B and p_C have already been discussed, while $p_S - p_B$ is predicted, and p_S and $p_R - p_B \equiv \delta p_R$ are prescribed. It remains to determine T_C and T_R. The former is obtained from

$$T_C = [h_M - gz_C - L(q + l)_M]/C_p, \quad \text{(A11)}$$

where

$$z_C = \delta z_M\left(\frac{p_S - p_C}{\delta p_M}\right) . \quad \text{(A12)}$$

Finally, we use

$$T_R = T_C + (T_C - T_B)\left(\frac{\delta p_R}{p_C - p_B}\right) . \quad \text{(A13)}$$

APPENDIX B

Evaluation of N and P

The purpose of this appendix is to explain the calculation of N and P, for use in the mixed-layer model described in Section 6.

The first step is the calculation of F_{sv} at levels S, $C-$, $C+$, R and B, using (3.16)–(3:17). We then obtain $P - N$, using

$$P - N \approx \tfrac{1}{2}\kappa\left\{(p_S - p_C)\left[\frac{(F_{sv})_S}{p_S} + \frac{(F_{sv})_{C-}}{p_C}\right] + (p_C - p_R)\left[\frac{(F_{sv})_{C+}}{p_C} + \frac{(F_{sv})_R}{p_R}\right] + (p_R - p_B)\left[\frac{(F_{sv})_R}{p_R} + \frac{(F_{sv})_B}{p_B}\right]\right\} . \quad \text{(B1)}$$

We now define

$$\xi_{SC} \equiv \begin{cases} 1, & \text{if } (F_{sv})_S \geq 0 \text{ and } (F_{sv})_C \geq 0 \\ \dfrac{(F_{sv})_S}{(F_{sv})_S - (F_{sv})_{C-}}, & \text{if } (F_{sv})_S > 0 \text{ and } (F_{sv})_{C-} < 0 \\ \dfrac{-(F_{sv})_{C-}}{(F_{sv})_S - (F_{sv})_{C-}}, & \text{if } (F_{sv})_S < 0 \text{ and } (F_{sv})_{C-} > 0 \\ 0, & \text{if } (F_{sv})_S < 0 \text{ and } (F_{sv})_{C-} < 0, \end{cases} \quad \text{(B2)}$$

$$\xi_{CR} \equiv \begin{cases} 1, & \text{if } (F_{sv})_{C+} \geq 0 \text{ and } (F_{sv})_R \geq 0 \\ \dfrac{(F_{sv})_{C+}}{(F_{sv})_{C+} - (F_{sv})_R}, & \text{if } (F_{sv})_{C+} > 0 \text{ and } (F_{sv})_R < 0 \\ \dfrac{-(F_{sv})_R}{(F_{sv})_{C+} - (F_{sv})_R}, & \text{if } (F_{sv})_{C+} < 0 \text{ and } (F_{sv})_R > 0 \\ 0, & \text{if } (F_{sv})_{C+} < 0 \text{ and } (F_{sv})_R < 0, \end{cases} \quad \text{(B3)}$$

$$\xi_{RB} \equiv \begin{cases} 1, & \text{if } (F_{sv})_R \geq 0 \text{ and } (F_{sv})_B \geq 0 \\ \dfrac{(F_{sv})_R}{(F_{sv})_R - (F_{sv})_B}, & \text{if } (F_{sv})_R > 0 \text{ and } (F_{sv})_B < 0 \\ \dfrac{-(F_{sv})_B}{(F_{sv})_R - (F_{sv})_B}, & \text{if } (F_{sv})_R < 0 \text{ and } (F_{sv})_B > 0 \\ 0, & \text{if } (F_{sv})_R < 0 \text{ and } (F_{sv})_B < 0. \end{cases} \quad \text{(B4)}$$

For completeness, we have allowed the possibility $(F_{sv})_B \geq 0$ in (B4), even though, as discussed in Section 3, this never actually happens in our model. It is easy to show that

$$P \approx \frac{1}{2}\kappa\left\{(p_S - p_C)\xi_{SC}\left[\frac{(F_{sv})_S}{p_S} + \frac{(F_{sv})_{C-}}{p_C}\right] + (p_C - p_R)\xi_{CR}\left[\frac{(F_{sv})_{C+}}{p_C} + \frac{(F_{sv})_R}{p_R}\right] + (p_R - p_B)\xi_{RB}\left[\frac{(F_{sv})_R}{p_R} + \frac{(F_{sv})_B}{p_B}\right]\right\}. \quad \text{(B5)}$$

Now that we have obtained both $P - N$ and P, we can use the identity $N = P - (P - N)$ to determine N.

REFERENCES

Ball, F. K., 1960: Control of inversion height by surface heating. *Quart. J. Roy. Meteor. Soc.*, **86**, 483–494.

Benoit, R., 1976: A comprehensive parameterization of the atmospheric boundary layer for general circulation models. Ph.D. dissertation, McGill University, and National Center for Atmospheric Research Cooperative thesis No. 39, 278 pp.

Deardorff, J. W., 1974: Three-dimensional numerical study of the height and mean structure of a heated planetary boundary layer. *Bound. Layer Meteor.*, **7**, 81–106.

——, 1976: On the entrainment rate of a stratocumulus-topped mixed layer. *Quart. J. Roy. Meteor. Soc.*, **102**, 563–582.

Herman, G., 1979: Thermal radiation in arctic stratus clouds. Submitted to *Quart. J. Roy. Meteor. Soc.*

——, and R. Goody, 1976: Formation and persistence of summertime arctic stratus clouds. *J. Atmos. Sci.*, **33**, 1537–1553.

James, D. G., 1959: Observations from aircraft of temperatures and humidities near stratocumulus clouds. *Quart. J. Roy. Meteor. Soc.*, **85**, 120–130.

Kahn, P. H., and J. A. Businger, 1979: The effect of radiative flux divergence on entrainment of a saturated convective boundary layer. *Quart. J. Roy. Meteor. Soc.*, **105**, 303–306.

Kraus, H., and E. Schaller, 1978: A note on the closure in Lilly-type inversion models. *Tellus*, **30**, 284–288.

Kuriyan, J. G., and S. K. Mitra, 1979: Window region IR radiation transfer through clouds and the sensitivity of cloud parameters to radiative effects. Accepted for publication in *J. Quant. Spectros. Radiat. Transfer.*

Lenschow, D. S., 1973: Two examples of planetary boundary layer modification over the Great Lakes. *J. Atmos. Sci.*, **30**, 568–581.

Lilly, D. K., 1968: Models of cloud-topped mixed layers under a strong inversion. *Quart. J. Roy. Meteor. Soc.*, **94**, 292–309.

——, and W. H. Schubert, 1980: The effects of radiative cooling in a cloud-topped mixed layer. *J. Atmos. Sci.*, **37** (in press).

Neiburger, M., 1949: Reflection, absorption, and transmission of radiation by stratus cloud. *J. Meteor.*, **6**, 98–104.

Oliver, D. A., W. S. Lewellen and G. G. Williamson, 1978: The interaction between turbulent and radiative transport in the development of fog and low-level stratus. *J. Atmos. Sci.*, **35**, 301–316.

Paltridge, G. W., 1974: Infrared emissivity, short-wave albedo, and the microphysics of stratiform water clouds. *J. Geophys. Res.*, **79**, 4053–4058.

Platt, C. M. R., 1976: Infrared absorption and liquid water content in stratocumulus clouds. *Quart. J. Roy. Meteor. Soc.*, **102**, 553–561.

Randall, D. A., 1976: The interaction of the planetary boundary layer with large-scale circulations. Ph.D. Thesis, The University of California, Los Angeles, 247 pp.

——, 1979: The entraining moist boundary layer. *Preprints Fourth Symp. Turbulence, Diffusion and Air Pollution*, Reno, Amer. Meteor. Soc., 467–470.

——, 1980: Conditional instability of the first kind upside-down. *J. Atmos. Sci.*, **37**, 125–130.

Schubert, W. H., 1976: Experiments with Lilly's cloud-topped mixed layer model. *J. Atmos. Sci.*, **33**, 436–446.

——, J. S. Wakefield, E. J. Steiner, and S. K. Cox, 1979: Marine stratocumulus convection, Part I: Governing equations and horizontally homogeneous solutions. *J. Atmos. Sci.*, **36**, 1286–1307.

Wakefield, J. S., and W. H. Schubert, 1976: Design and execution of the marine stratocumulus experiment. Atmos. Sci. Pap. No. 256, Colorado State University, 74 pp.